

Opening review: The GPS and CSS Sources: Issues and Opportunities

Chris O'Dea (U Manitoba)

Based on the review paper O'Dea & Saikia 2021,
A&A Rev.

Thanks to all who contributed figures, references,
and comments!

Outline

Major Recent Developments (Highlights)

Open Issues and Next Steps

Recent Developments

More samples.

More key data: HI, CO, IR, X-ray, Gamma ray.

Better understanding of central engine properties.

Jet-induced star formation?

Possible relations to other populations (NLS1, FR0).

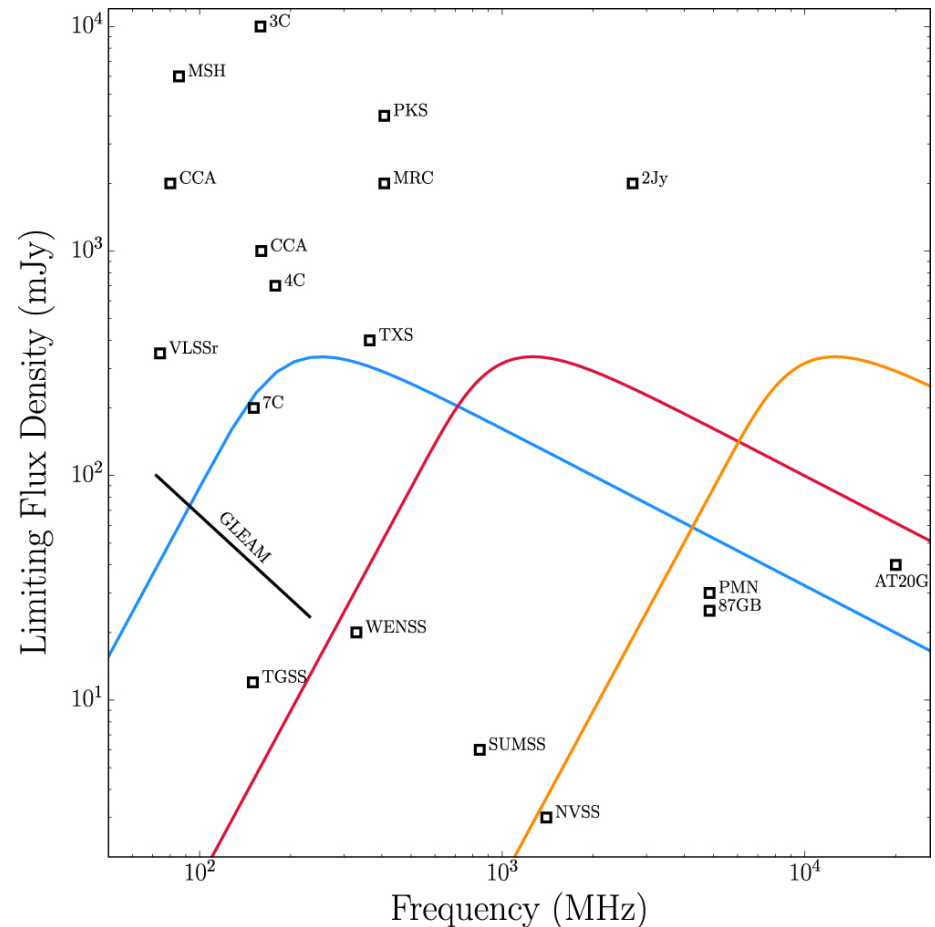
Stronger evidence for Radio Jet Feedback.

You will hear about these during the meeting, so I will just give a few highlights.

New samples include thousands of PS and CSS sources (e.g., Callingham+ 2017)

The new samples cover a broader range of frequency (Callingham+ 2017, Hancock+2009) and extend down to lower radio power.

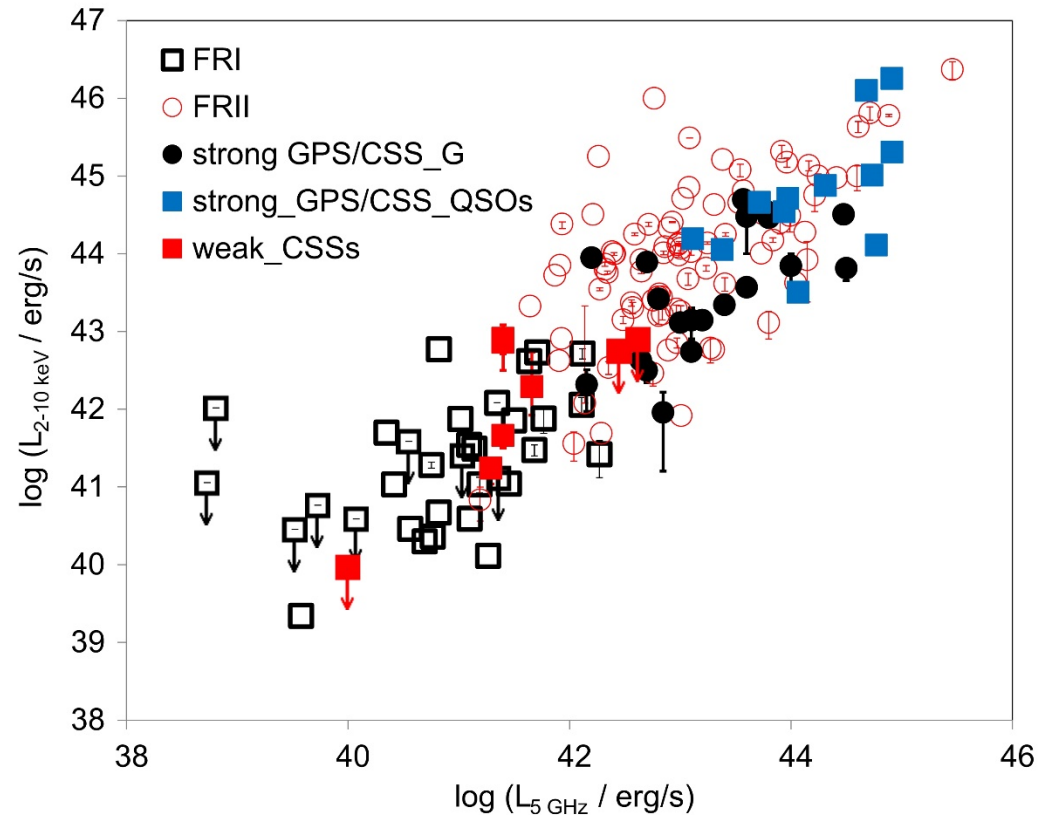
PS can have narrow spectra, so a range of wavelengths is required.



Comparison of parameter space of various radio surveys. (Callingham+2017).

X-ray – Radio Relations

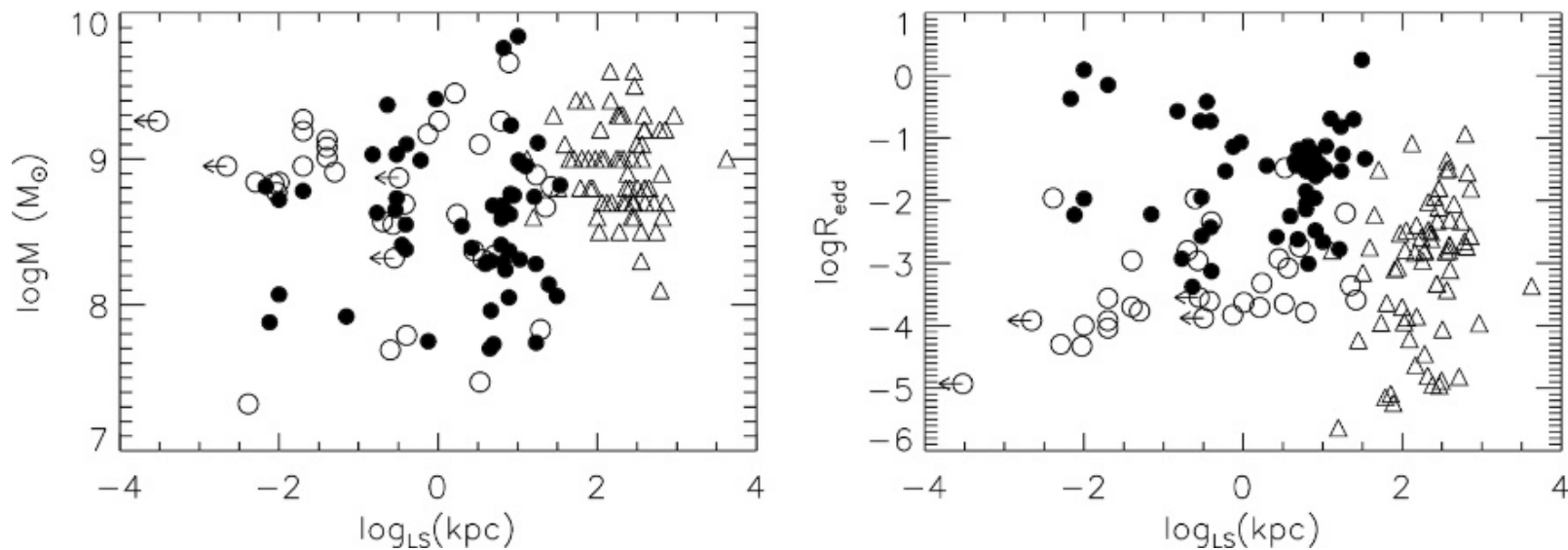
There is a continuity of properties along the X-ray - radio relationship.



2--10 keV luminosity vs. 5 GHz luminosity for GPS, CSS, FRI and FRII radio sources from Kunert-Bajraszewska + (2014). Strong and weak refer to high and low radio power, respectively.

Compact and Large Sources have overlap in BH Mass and Eddington Ratio

There is a group of compact sources with BH Masses less than 10^8 solar masses which are not seen in the larger sources. These objects with smaller BH mass are unlikely to become the large sources.

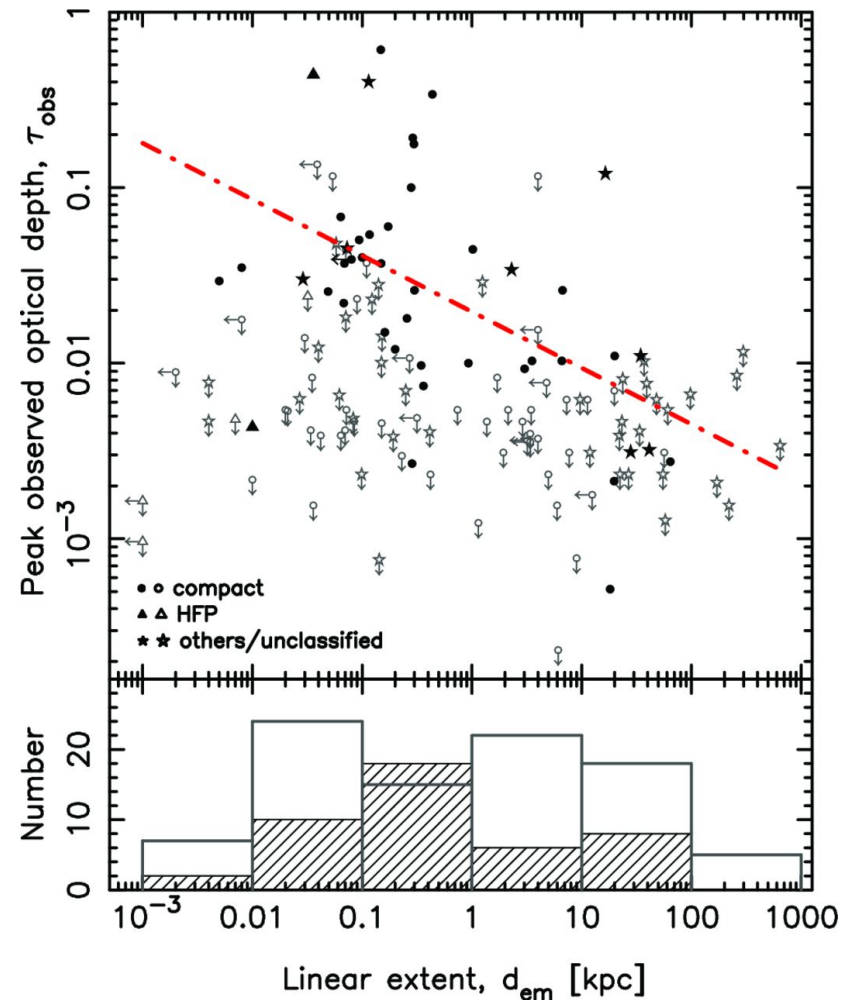


(Left) BH mass versus radio source linear size (LS). (Right) Eddington ratio versus LS. The filled and open circles are young radio AGNs in the Liao & Gu (2020) sample classified as quasar and galaxy, respectively. The triangles are large-scale radio galaxies in Hu + (2016), used as comparison. The arrows represent the upper limits on the LS. (From Liao & Gu 2020).

Atomic Hydrogen in Compact Sources

Overall, the HI detection rate of compact sources is about twice that of the extended sources (32% vs. 16%, e.g. Maccagni +2017).

Peak optical depth is higher in compact sources (Curran+2013).



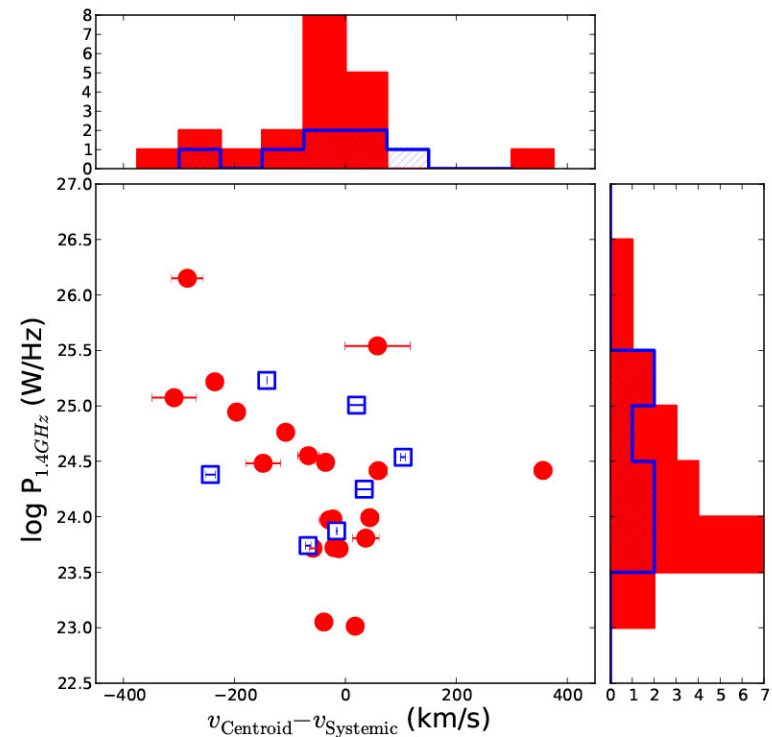
The peak observed optical depth versus the projected linear size (where available) for all of the redshifted radio sources searched in 21-cm absorption to date (compiled in Curran & Whiting 2010; Allison et al. 2012). The filled markers/hatched histogram represent the detections and the unfilled markers/histogram show the 3σ upper limits to the optical depth for the non-detections at a spectral resolution of 167 km/s (see Curran et al. 2013a). The circles designate compact objects and the stars non-compact/unclassified, with the triangles showing the high-frequency peaker galaxies, which, although compact, Orienti et al. (2006) argue do not follow the trend. The line shows the least-squares fit to the detections. (Curran + 2013).

Statistics of Outflows in Compact Sources

22% (15/68) of sources with [OIII] detected in SDSS spectra show blue wings in [OIII] (Liao & Gu 2020). Higher fraction (71%) seen by Holt+2008.

About 23% of compact sources with an HI absorption detection show a blue wing in the HI with an outflow velocity > 100 km/s (Maccagni+2017, Morganti & Osterloo 2018).

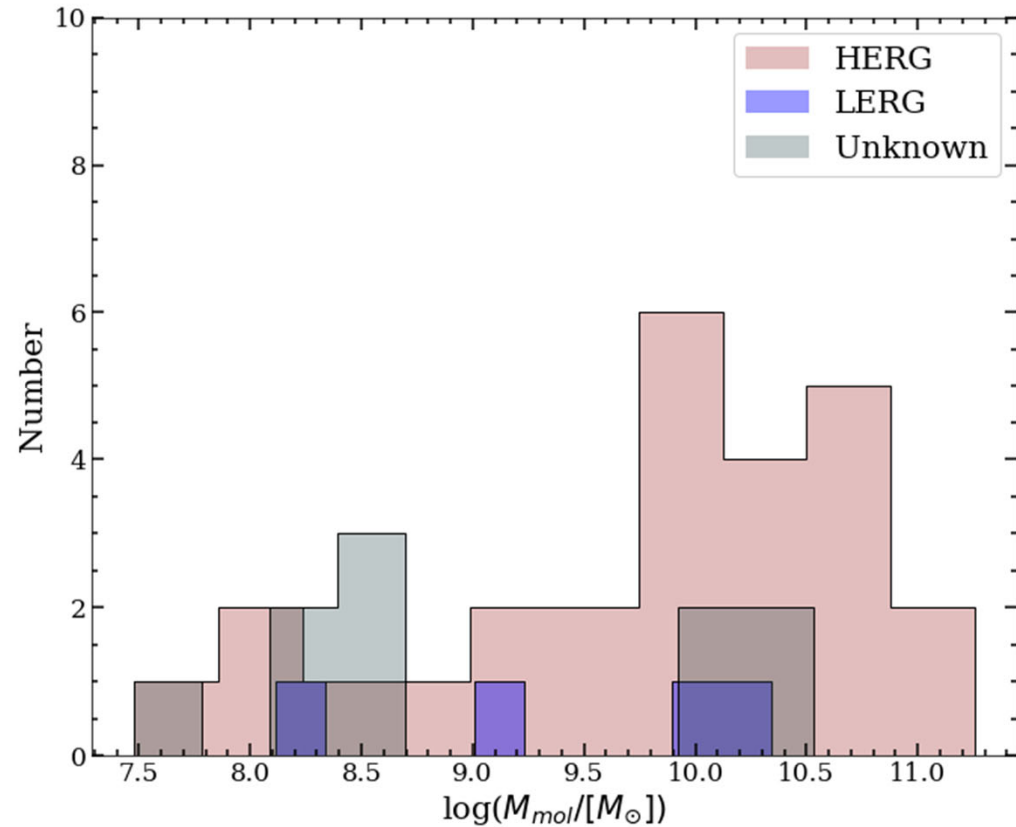
Blue wings in HI absorption occur above a minimum radio power of 10^{24} W/Hz (Gereb+2015).



Blueshift/redshift distribution of the H I line centroid vs. the radio power of compact (red circles) and extended sources (blue empty squares). (Gereb+2015).

Molecular Gas Content

Some compact sources have substantial amounts of molecular gas.

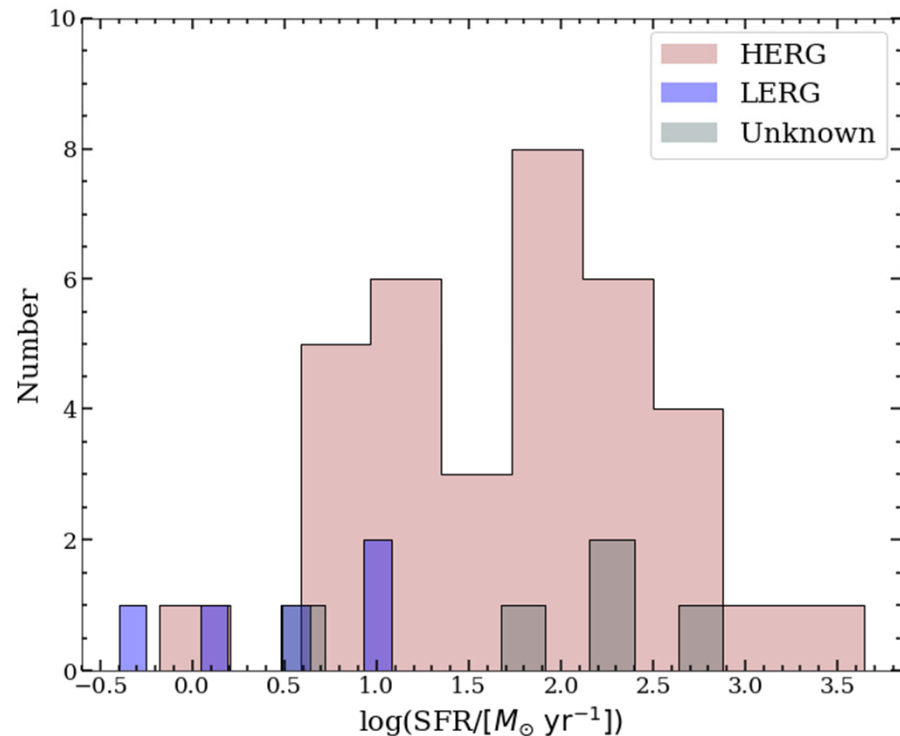


Mass of molecular gas from CO, dust, and X-ray N_{H} . If there are more than one estimate for a given source, the estimates were averaged. The values are shaded using the emission line class (HERG/LERG). (O'Dea & Saikia 2021).

Star Formation Rates (SFR)

Some compact sources have substantial SFR ranging from tens to hundreds of solar masses per year.

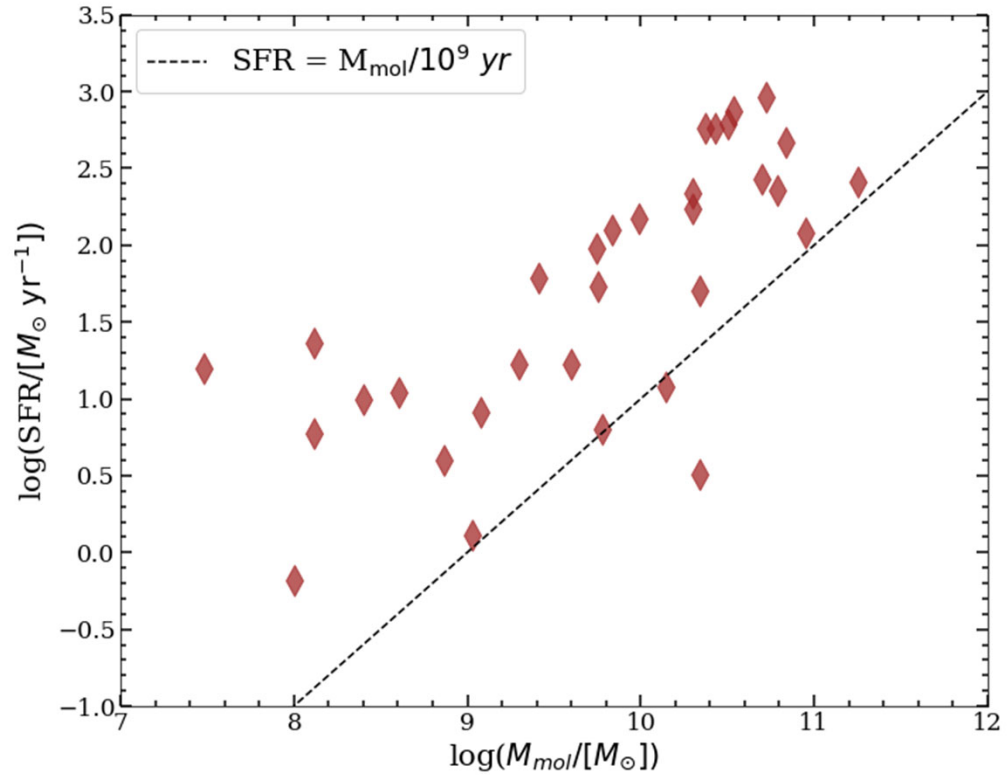
Several studies suggest that compact sources are more likely to have significant star formation than large sources (Tadhuner+2011, Dicken+2012, Ogle+2021).



SFR from PAH or FIR luminosity.. If there are more than one estimate for a given source, the estimates were averaged. The values are shaded using the emission line class (HERG/LERG). (O’Dea & Saikia 2021)

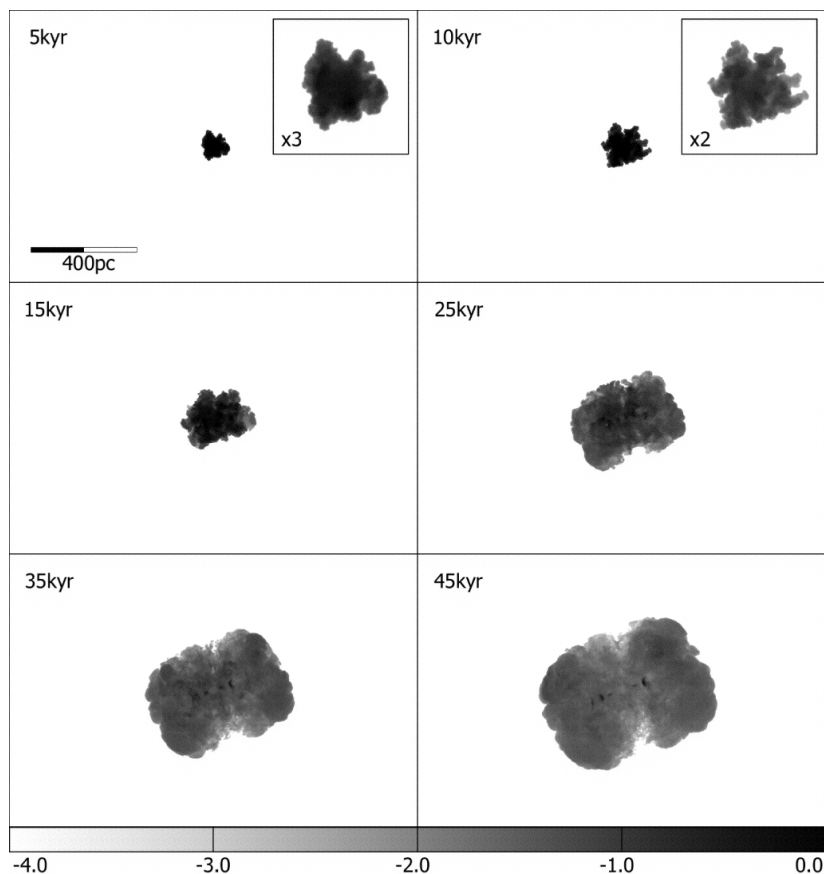
Star Formation is enhanced in Compact Sources.

The compact sources have a higher rate of star formation for a given molecular gas mass than normal star forming galaxies.

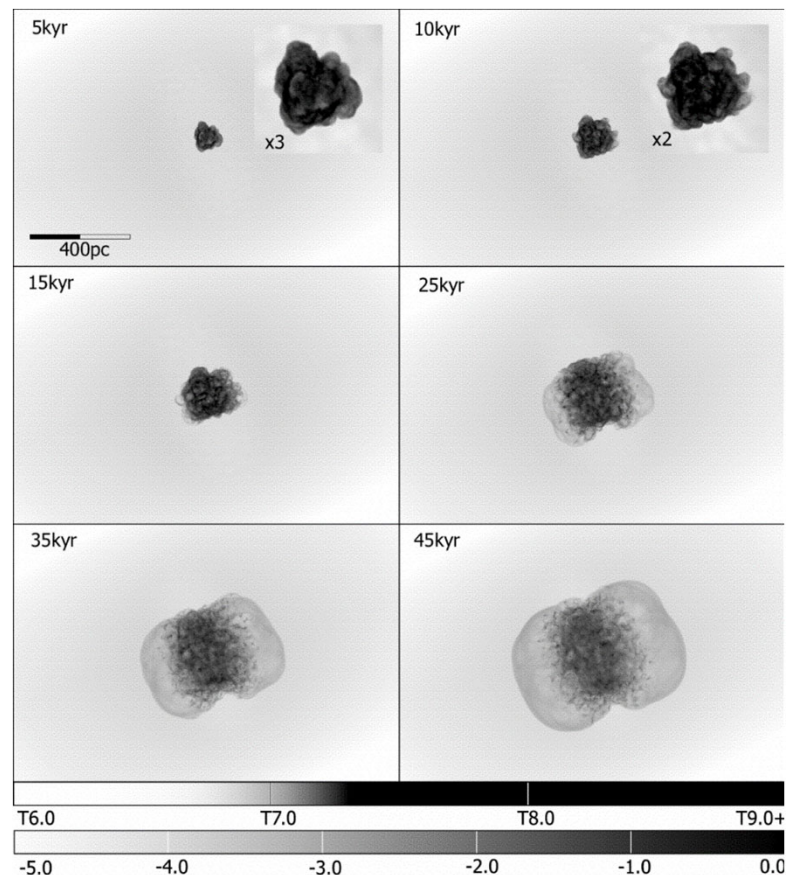


SFR is shown against the mass of molecular gas. If there are more than one estimate for a given source, the estimates were averaged. The SFR lie above a line which assumes a gas depletion time scale of 10^9 yr which is typical of normal galaxies. This indicates that the PS and CSS sources have enhanced star formation relative to normal star forming galaxies. (O’Dea & Saikia 2021).

Alignment of Radio and X-ray Emission from Simulations



(Left) Radio surface brightness: The panels represent the logarithm of the synthetic radio surface brightness at the 5–45 kyr phases of the evolution. (Sutherland & Bicknell 2007)

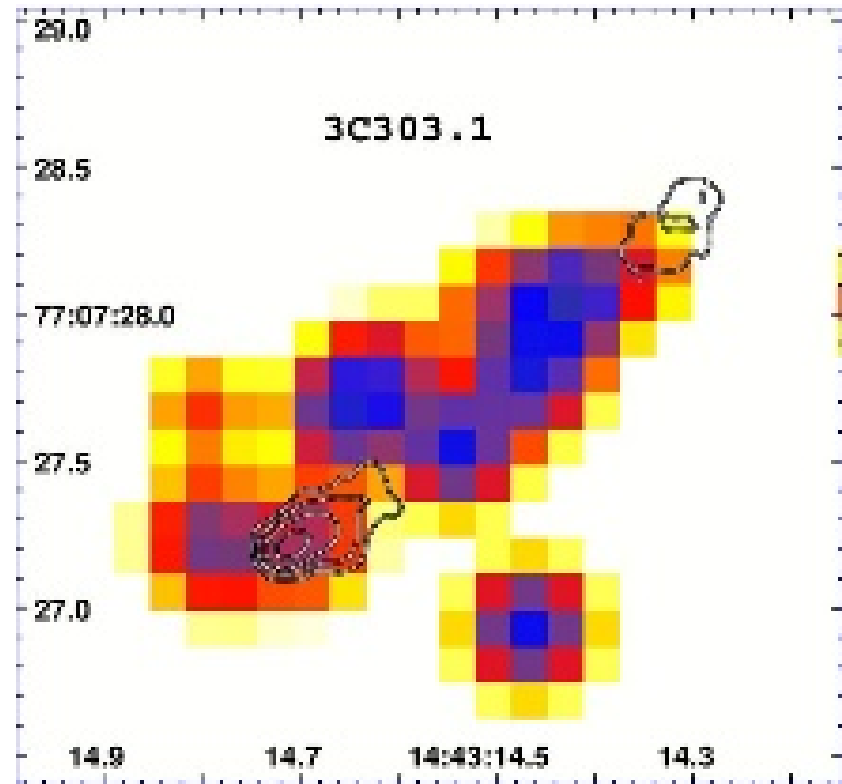


(Right) Hard X-rays (1.5 – 10 keV): Logarithm of the hard X-ray surface brightness between 5 and 45 kyr. The upper gray-scale bar with numbers prefixed by "T" indicates the relative contribution of gas at various temperatures to the emissivity. Dark indicates a large contribution; light indicates a low contribution. (Sutherland & Bicknell 2007)

X-rays from Hot, Shocked Gas in 3C303.1

X-ray emission is aligned
along the radio source axis
in 3C303.1 (Massaro + 2010).

XMM-Newton X-ray
spectroscopy shows the
emission is consistent with
hot, shocked gas (O'Dea +
2006).

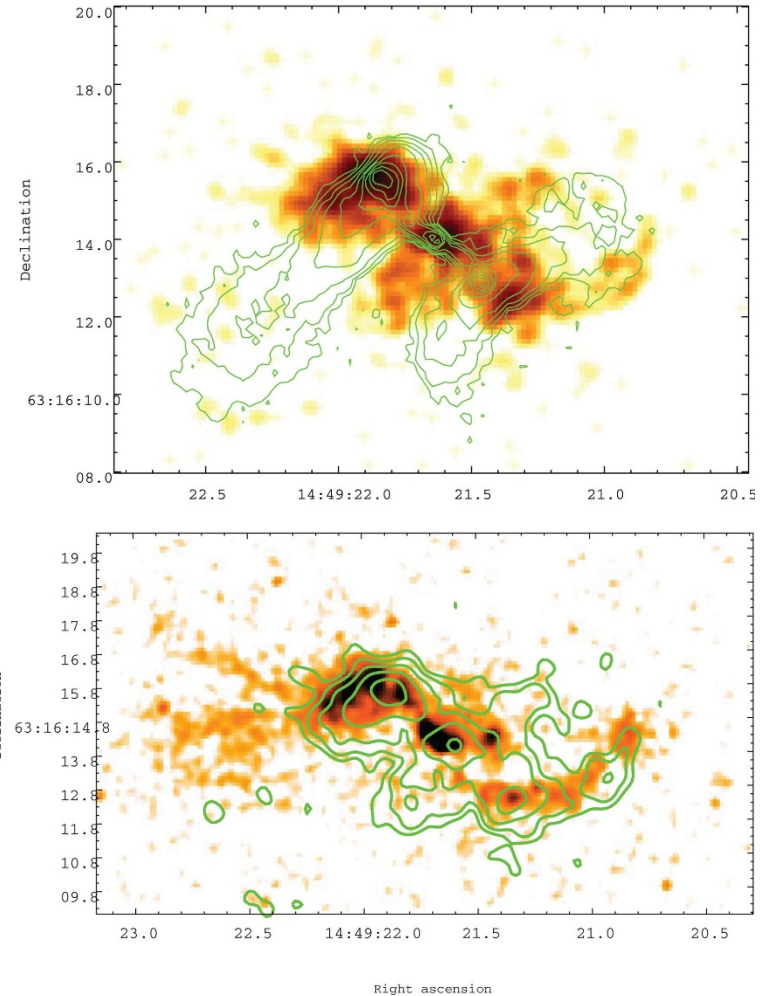


3C 303.1. Chandra Flux map rebinned by a factor of 4 to give smaller pixel size, FWHM = 0.25". 5.0 GHz radio contours: 1 mJy/beam, increasing by factors of 4. (Radio map available on the Merlin archive.) Note X-ray is aligned along radio axis. (Massaro +2010).

Shocked Gas in 3C305

In 3C305, the X-ray emission is aligned with both the radio and the [OIII] emission line (Massaro +2009, Balmaverde +2012, Hardcastle +2012).

X-ray spectroscopy indicates the X-rays are produced by hot, shocked ISM (Hardcastle + 2012).

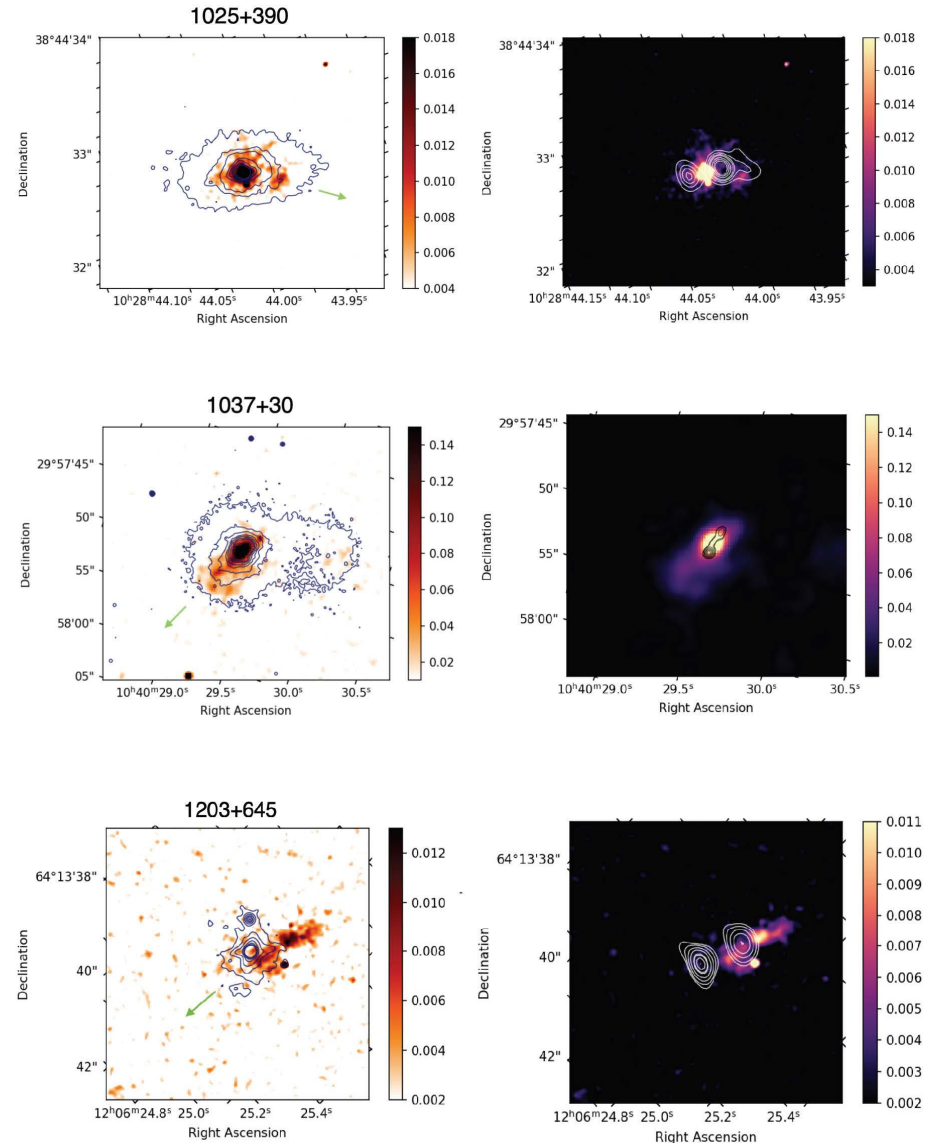


(Top) Radio and X-ray image of 3C 305. Contours are from the 8-GHz image. The colours show the Chandra data in the 0.5–5.0 keV band, binned in pixels of 0.123 arcsec on a side and smoothed with a Gaussian of full width at half-maximum (FWHM) 3 pixels; the smoothed Chandra image has an effective resolution of ~ 0.6 arcsec.
(Bottom) [O III] and X-ray image of 3C 305. Contours show the 0.5–5.0 keV X-ray emission, binned and smoothed as in top: the lowest contour is the 3σ surface-brightness level, relative to the off-source background, and each successive contour is a factor of 2 higher in surface brightness. The colours show the [O III] 500.7-nm image of Privon +(2008), smoothed with a Gaussian of FWHM 2 pixels to improve surface-brightness sensitivity. (Hardcastle +2012).

Jet-Induced Star Formation?

HST UV images show that UV light is often aligned with the radio source in CSS (Duggal + 2021).

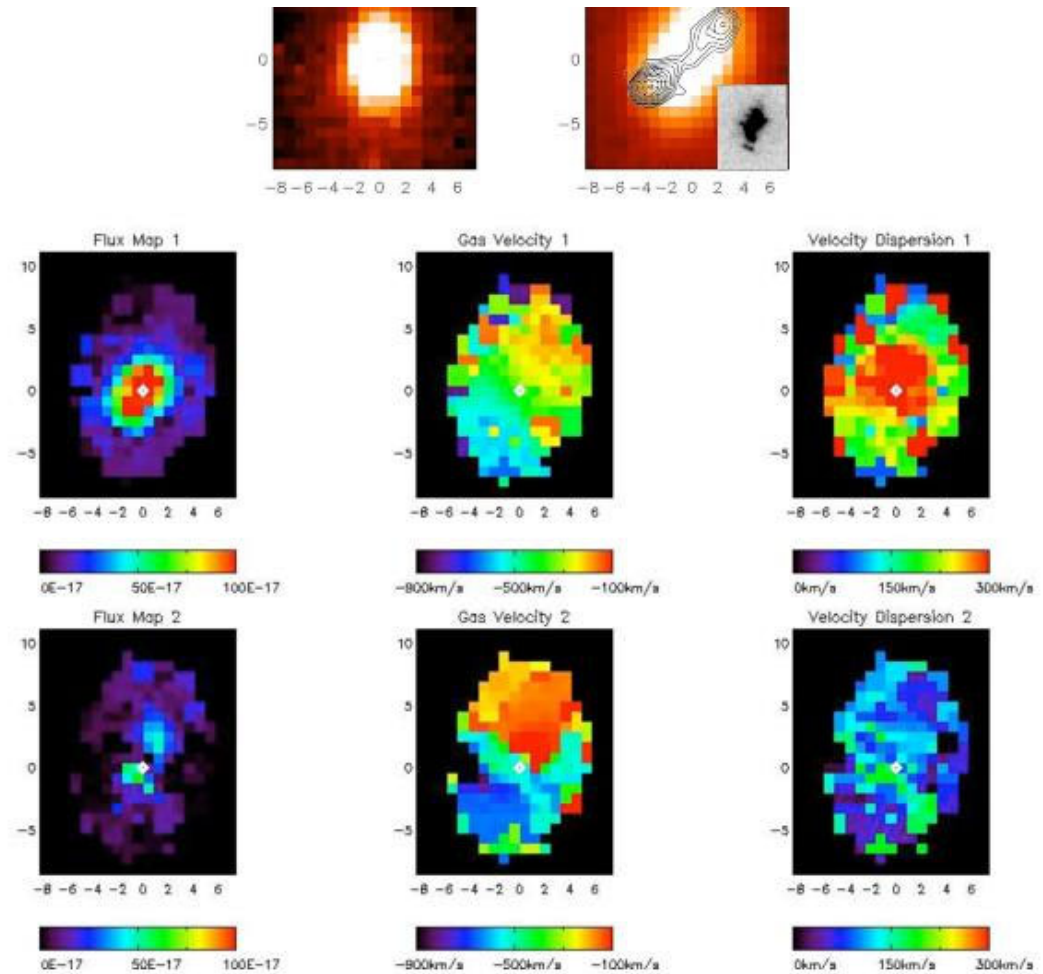
If other mechanisms can be ruled out (scattered nuclear light, nebular continuum) this would provide evidence for jet-induced star formation.



Left panels: HST optical image (contours) over layed with UV images (color). Right panels: Radio image (contours) over layed with UV images (color). (Duggal +2021).

Kinematics of Shocked Gas in 3C303.1

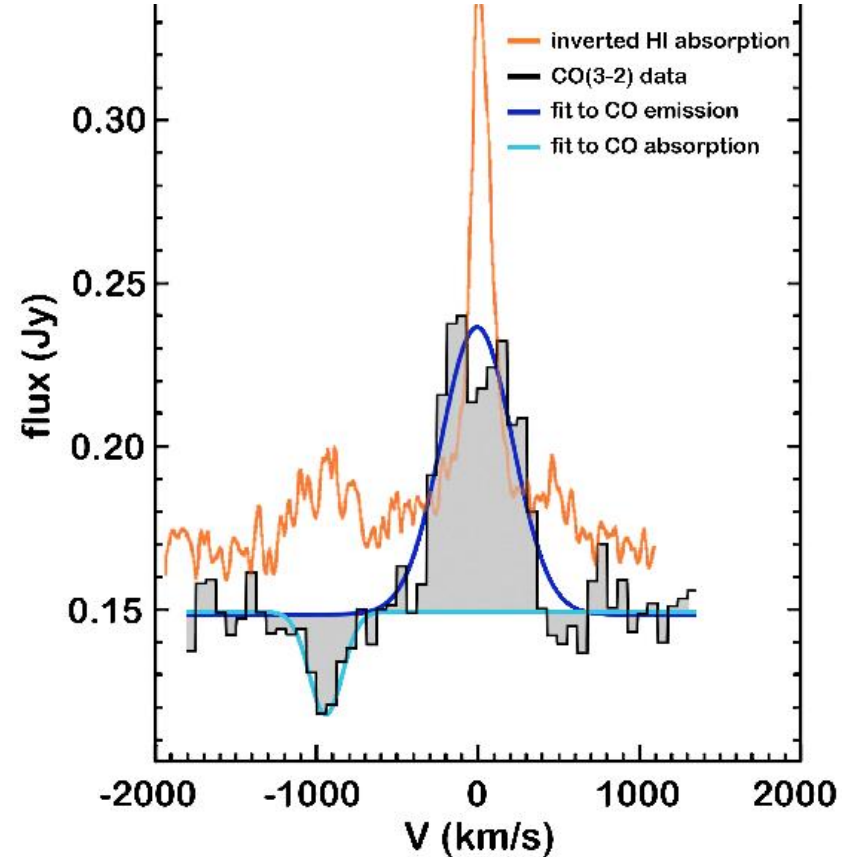
There is a velocity gradient along the radio axis for both the narrow and broad components as expected if the gas has been shocked by the expanding radio source (O'Dea + 2002, Holt + 2008, Shih +2013).



3C 303.1. (Top row): left—host galaxy image; right—[O III] image with MERLIN 8.4 GHz radio image from Akujor & Garrington (1995) overlaid. The inset on the right panel is the HST image published in Axon + (2000), the physical size of the inset is the same as the FOV of our data cube. (Middle row): left—flux map for the broad velocity component; middle—velocity map of the broad velocity component; right—velocity dispersion map of the broad velocity component. (Bottom Row): same as middle row but for the narrow velocity component. This image and all following images are oriented with north up and east to the left. (Shih + 2013).

Multi-phase Gas Outflow in 4C12.50

Molecular gas traced by
CO(3-2) and atomic
hydrogen (21 cm line)
show similar kinematics
(Dasyra & Combes 2012).

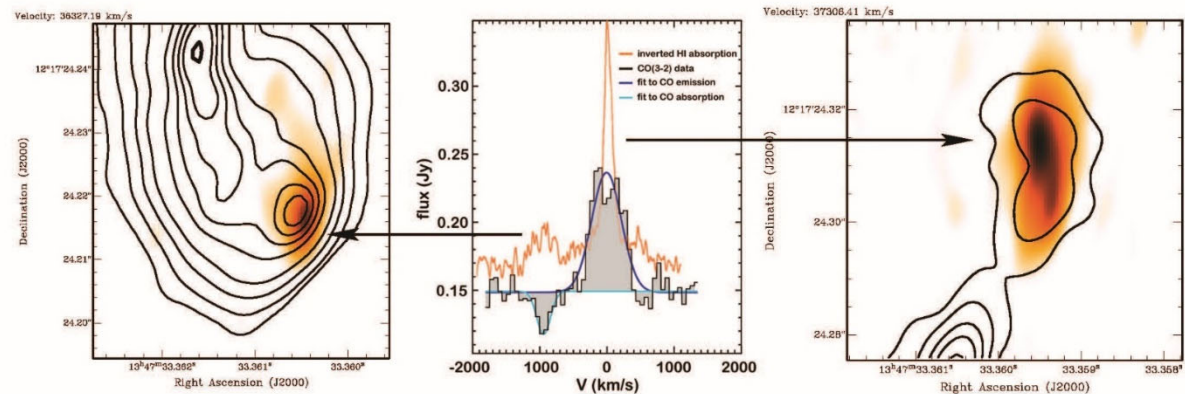


Flux-calibrated line profile of $^{12}\text{CO}(3-2)$, averaged over the WILMA and the FTS data to be least affected by potential artifacts. Gaussian functions with parameters that most closely fit the emission component at the systemic velocity and the absorption component at -950 km s^{-1} are shown in blue and cyan, respectively. The inverse Hi absorption that is seen in the radio data of 4C 12.50 (Morganti + 2004) is overplotted in orange for an arbitrary scale and continuum level. (Dasyra & Combes 2012).

Multi-phase Gas Outflow in 4C12.50

HI components are spatially separated. Systemic component is at northern lobe and blue shifted HI is at end of southern lobe. (Morganti +2013).

Fast HI outflow is apparently driven by the southern radio hot spot. (Morganti +2013).



The distribution of the H I absorption (orange–white) in two velocity channels for the source 4C 12.50, superimposed to the continuum emission (contours) showing the location of the two H I clouds detected in absorption (from Morganti + 2013). The inverted integrated H I absorption profile is shown in the central panel and clearly shows a strong, blueshifted H I outflow of ~ 1000 kms $^{-1}$ (from Morganti + 2005a). The cloud shown in the right panel has a narrow absorption profile near the systemic velocity, while the left panel shows the location of H I absorption associated with the fast H I outflow, co-spatial (in projection) with the bright radio hot spot. Also shown is the CO profile (taken from Dasyra and Combes 2012 which shows that a very similar outflow is detected in CO absorption. (Morganti & Osterloo 2018)

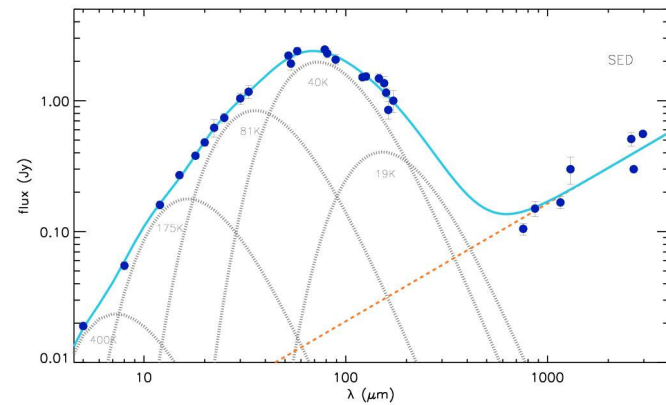
Outflow Energetics & Efficiencies

The best studied case 4C 12.50 is discussed by Dasyra+2014.

Most of mass flow is in molecular gas which has been heated up to 400 K.

Estimated KE of molecular gas is $\sim 10^{44}$ erg/s.

Estimated jet power is $\sim 3 \times 10^{45}$ ergs/s, so $\sim 3\%$ of jet power goes into accelerating molecular gas.



Dust SED of 4C12.50 including continuum measurements from the new IRAM and Herschel data. The modified black body curves (with temperatures between 19 K and 400 K) that best fit the IR/sub-mm data are plotted with dotted lines. The dashed line is a synchrotron – related power law with an exponent of 0.9. The solid line corresponds to the sum of the flux of all components. (Dasyra +2014)

Origin Stories*

Youth: Some could be younger versions of the large radio sources and will propagate out to larger scales over their active lifetimes.

Intermittent: Some could have short life times. These will turn off and fade before getting to large sizes.

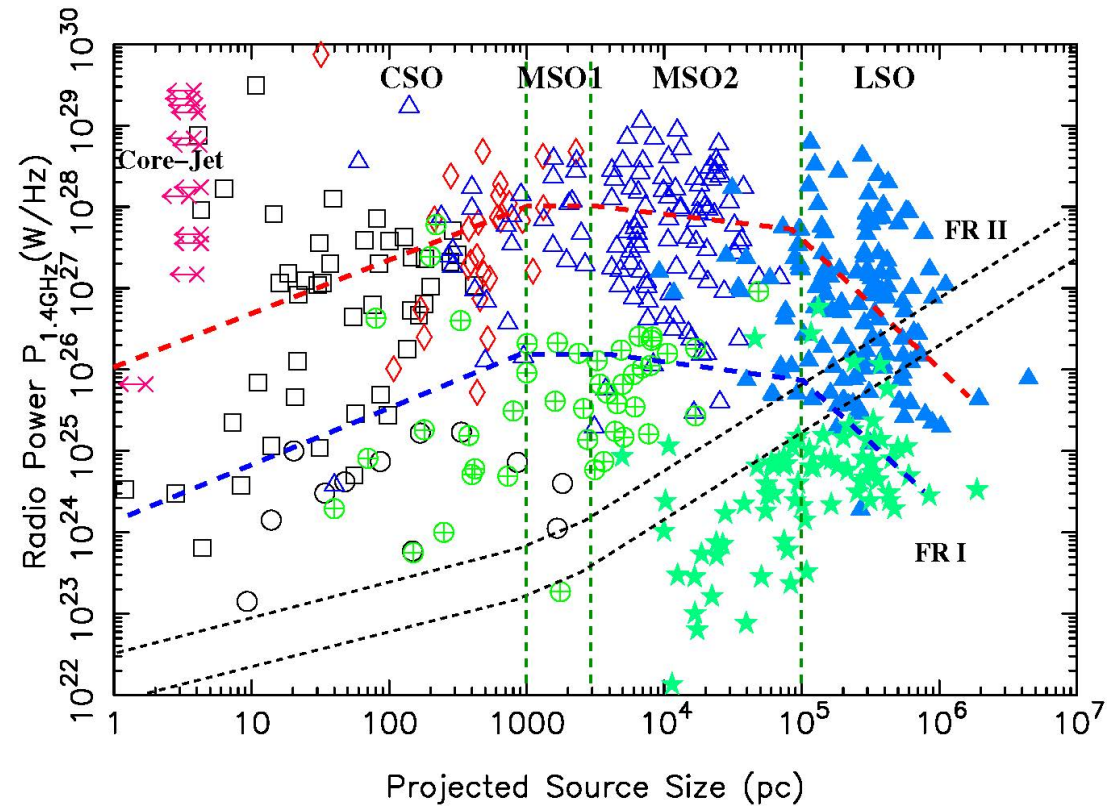
Frustration: Some could be stuck on small scales via interaction of the jets with dense gas clouds.

Imposters: Some might be in dense environments (like the frustrated sources), but the jet-cloud interaction enhances the radio emission. So these are intrinsically weaker sources which will never become large powerful radio sources. The dense gas clouds could also form stars, so these could also have enhanced star formation.

* Thanks to Stan Lee

Analytical Models Predict Trajectory on Power-Size Plane

Analytical models suggest that compact sources could evolve to become the large radio galaxies (e.g., Baldwin 1982, Fanti + 1995, Readhead +1996, O’Dea & Baum 1997, Snellen + 2000, An & Baan 2012).



Radio power vs. the linear extent of large-scale radio sources: compact, medium-sized, and large symmetric objects. Exemplary evolutionary tracks based on parametric modeling are depicted for the high-radio-power and low-radio-power sources using red and blue dashed lines. The black dashed lines mark the (approximate) boundary between stable laminar jet flows (above the lines) and unstable turbulent flows (below the lines). Symbols represent different morphological and spectral classes of radio sources. (An & Baan 2012).

Young (and Growing) Radio Galaxies

Pro:

Same host galaxies.

Continuity of AGN Properties.

Proper Motions.

Plausible evolution scenarios.

There must be progenitors of the large sources.

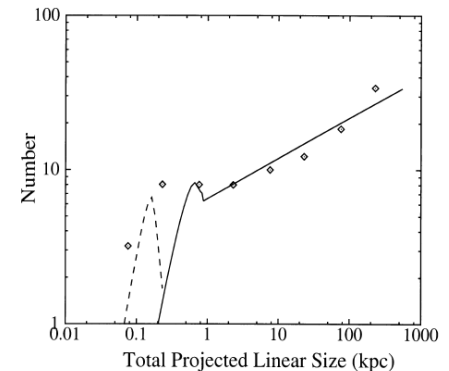
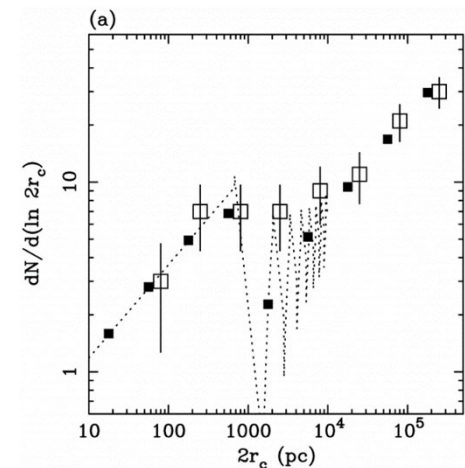
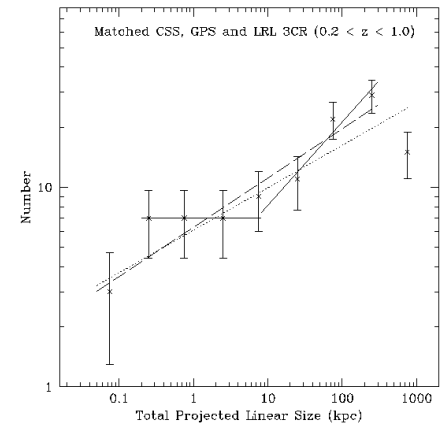
Con:

Too many small sources, so not all can become large sources

There's too many of them

- Over the entire range $N \sim L^{0.25}$
- There is a flattening at small size (O'Dea & Baum 1997)
- Models which fit the data include
 - Intermittent sources (Reynolds & Begelman 1997)
 - A subpopulation which is disrupted on small scales (Alexander 2000)

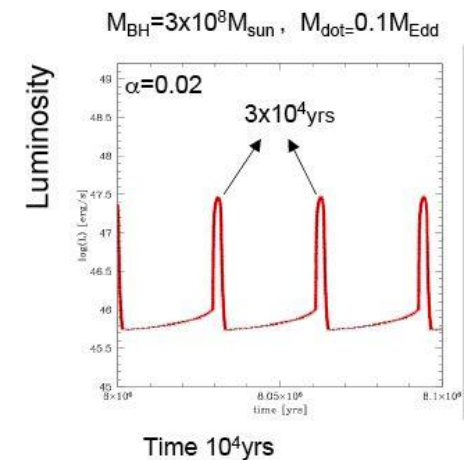
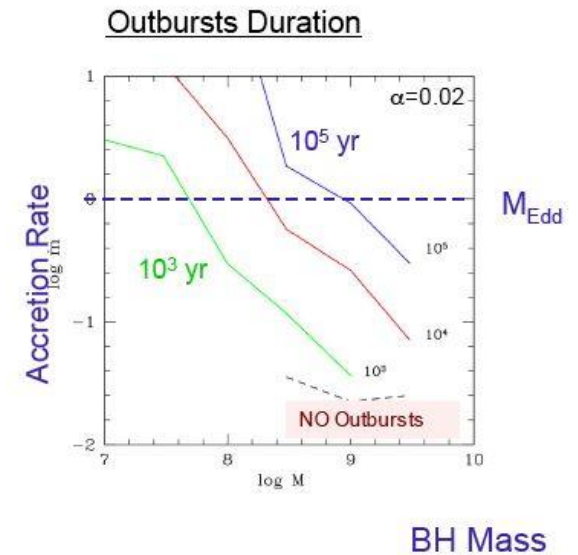
(Top) data from the GPS, CSS, and LRL samples (O'Dea and Baum (1997, see also Fanti 2008) (Middle) Fit to the data which includes intermittent radio sources (Reynolds & Begelman 1997). (Bottom) Fit to the data which includes sources which disrupt on small scales (Alexander 2000).



Accretion Disk Instabilities as a Driver of Intermittency

A radiation pressure instability can cause variations in AGN activity with the relevant time scales (Czerny + 2009, Seimignoska + 2010).

X-ray AGN without emission line nebulae argue for timescales $\sim 10^5$ yr (Schawinski +2015).



Left: Luminosity variations due to the radiation pressure instability in an accretion disk around $M_{\text{BH}} = 3 \times 10^8 M_{\odot}$ and $\dot{M} = 0.1 \dot{M}_{\text{Edd}}$.

Right: Outburst durations represented as constant lines in the black hole mass vs. accretion rate parameter space. Outbursts lasting for 10^3 years are too short for the expansion of a radio source beyond its host galaxy. (Seimignowska + 2010).

Transient (short-lived) Sources

Pro:

It would provide a solution to the numbers problem.

Some evidence for short-time scale behavior in AGN.

Examples of candidate sources which have turned off.

Con:

Physical basis for short-lifetimes not yet understood.

Frustrated

Pro:

Evidence for strong interaction between radio source and environment (radio source asymmetry, alignment effect)

Evidence for massive cold ISM in some sources

Con:

Only some objects have massive cold ISM, but could explain some objects

Imposters

Pro:

Evidence for strong interaction of radio source with environment (radio source asymmetry, alignment effect)

Evidence for enhanced star formation in compact sources

Con:

Enhancement of radio power not well understood.

Complicated scenario.

Next Steps/Opportunities

Which of the origin stories are correct and what do they tell us about radio source physics? Larger samples (well selected) are needed to do source statistics properly and constrain origin and evolution.

What role do the PS and CSS sources play in radio mode feedback? We need studies of multi-phase outflows in many objects.

More ALMA CO observations could clarify amount and distribution of molecular gas and interaction with radio source.

Further gamma ray detections could help constrain the physics.

Numerical simulations can shed light on how the sources interact with their environment.

High redshift objects can constrain impact at Cosmic Noon.

Thank you!